USGS
science for a changing world

Radionuclide Data and Calculations and Loss-On-Ignition, X-Ray Fluorescence, and ICP–AES Data from Cores in Catchments of the Animas River, Colorado

Data Series 382

U.S. Department of the Interior
U.S. Geological Survey

Radionuclide Data and Calculations and Loss-On-Ignition, X-Ray Fluorescence, and ICP–AES Data from Cores in Catchments of the Animas River, Colorado

By Stanley E. Church, Cyndi A. Rice, and Marci E. Marot

Data Series 382

U.S. Department of the Interior
U.S. Geological Survey

U.S. Department of the Interior
DIRK KEMPTHORNE, Secretary

U.S. Geological Survey
Mark D. Myers, Director

U.S. Geological Survey, Reston, Virginia: 2008

For product and ordering information:
World Wide Web: http://www.usgs.gov/pubprod
Telephone: 1-888-ASK-USGS

For more information on the USGS--the Federal source for science about the Earth, its natural and living resources, natural hazards, and the environment:
World Wide Web: http://www.usgs.gov
Telephone: 1-888-ASK-USGS

Suggested citation:
Church, S.E., Rice, C.A., and Marot, M.E., 2008, Radionuclide data and calculations and loss-on-ignition, X-ray fluorescence, and ICP–AES data from cores in catchments of the Animas River, Colorado: U.S. Geological Survey Data Series 382, 20 p.

Contents

Introduction.....1
- Methods of Study.....3
  - Depositional Site Characteristics.....3
- Sample Collection.....3
  - Sediment Cores.....3
- Sample Preparation.....4

Analytical Methods and Results.....4
- Geochemical Analyses.....4
  - Trace-Element Analysis by Inductively Coupled Plasma–Atomic Emission Spectrometry.....4
  - X-Ray Fluorescence Analysis.....4
  - Radionuclide Analysis.....10
  - ^{210}Pb Radiometric Calculations.....15
  - Geochemical Influence of Periodic Flooding of the Oxbow Lakes, Durango Area.....17

References Cited.....19

Figures

1. Map of the Animas River watershed, Colorado, showing relationship of two detailed study areas to Animas River.....1
2. 1973 aerial photograph showing localities sampled in oxbow lakes, Durango, Colorado.....2
3. 1973 aerial photograph showing localities of sampled abandoned beaver ponds, Mineral Creek drainage, Colorado.....3

4–6. ^{210}Pb decay curve for:

4. Core 99928-1.....15
5. Core 99929-2.....16
6. Core 99929-3.....16

Tables

1. Sample localities and data on cores, Animas River watershed, Colorado.....4

2–6. Core descriptions, depths, and geochemical data from:

2. Core 99928-1.....5
3. Core 97ABS300.....6
4. Core 99929-1.....7
5. Core 99929-2.....8
6. Core 99929-3.....9

7–10. Sample depths, loss-on-ignition, radionuclide activity, flux, and inventory data and ^{210}Pb age calculations for:

7. Core 99928-1.....11

8. Core 99929-1 12
9. Core 99929-2 13
10. Core 99929-3 14
11. Discharge records from NWIS gage 09361500, 32nd St. Bridge, Durango, Colo 18

Radionuclide Data and Calculations and Loss-On-Ignition, X-Ray Fluorescence, and ICP–AES Data from Cores in Catchments of the Animas River, Colorado

By Stanley E. Church, Cyndi A. Rice, and Marci E. Marot

Introduction

The U.S. Departments of Agriculture and Interior (USDA–DOI) Abandoned Mine Lands (AML) Initiative is focused on the evaluation of the effect of past mining practices on the water quality and the riparian and aquatic habitats of impacted stream reaches downstream from historical mining districts located primarily on Federal lands. This problem is manifest in the eleven western states (west of longitude 102°) where the majority of hardrock mines that had past production are located on Federal lands (Ferderer, 1996; USDA Forest Service and Bureau of Land Management, 2007). In areas of temperate climate and moderate to heavy precipitation, the effects of rapid chemical and physical weathering of sulfides exposed on mine-waste dumps and acidic drainage from mines have resulted in elevated metal concentrations in the stream water and stream-bed sediment. The result of these mineral weathering processes has an unquantified impact on the quality of the water and the aquatic and riparian habitats that may limit their recreational resource value. One of the confounding factors in these studies is the determination of the component of metals derived from hydrothermally altered but unmined portions of these drainage basins (Runnells and others, 1992).

Several watersheds have been studied to evaluate the effects of acid mine drainage (AMD) and acid rock drainage (ARD) on the near-surface environment (U.S. Geological Survey, 1997). The Animas River watershed in southwestern Colorado (fig. 1) contains a large number of past-producing metal mines (Church and others, 2007) that have affected the watershed. Beginning in October 1996, the U.S. Geological Survey (USGS) began a collaborative study of these effects under the USGS-AML Initiative (Buxton and others, 1997). In this report, we present the radionuclide and geochemical analytical results of sediment coring during 1997–1999 from two cores from oxbow lakes 0.5 mi. upstream from the 32nd Street Bridge near Durango, Colo. (fig. 2), and from three cores from beaver ponds within the Mineral Creek drainage basin near Silverton, Colo. (fig. 3).

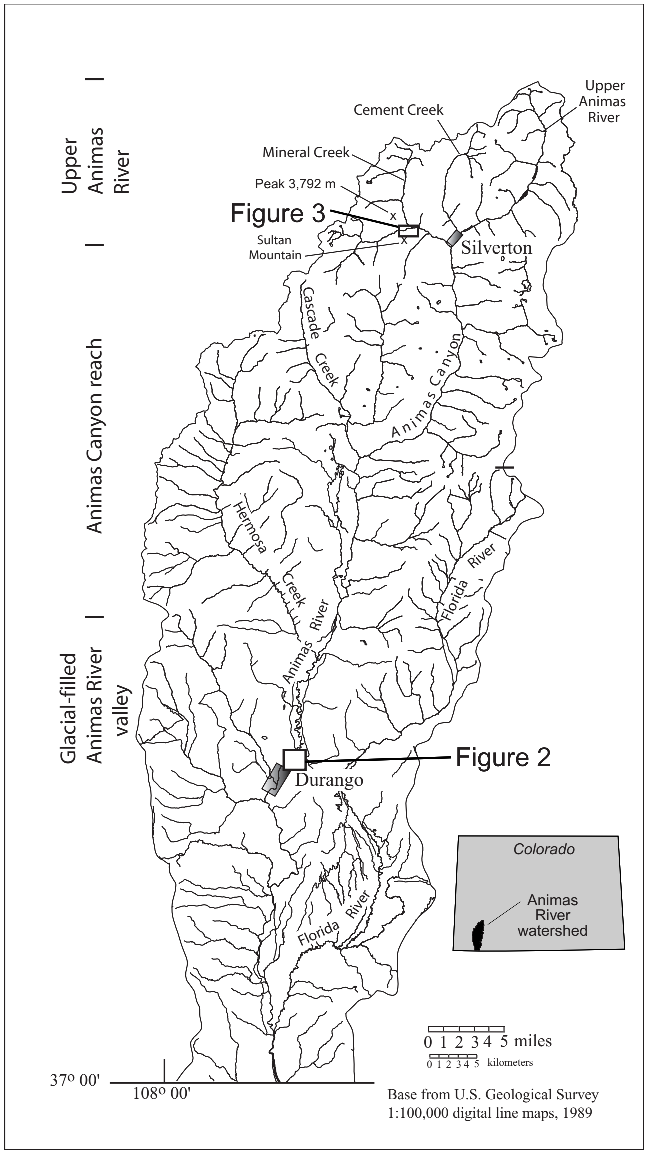

Figure 1. Map of the Animas River watershed in Colorado showing the relationship of the mineralized headwaters area of the watershed north of Silverton to areas studied near Durango (fig. 2) and Mineral Creek west of Silverton (fig. 3).

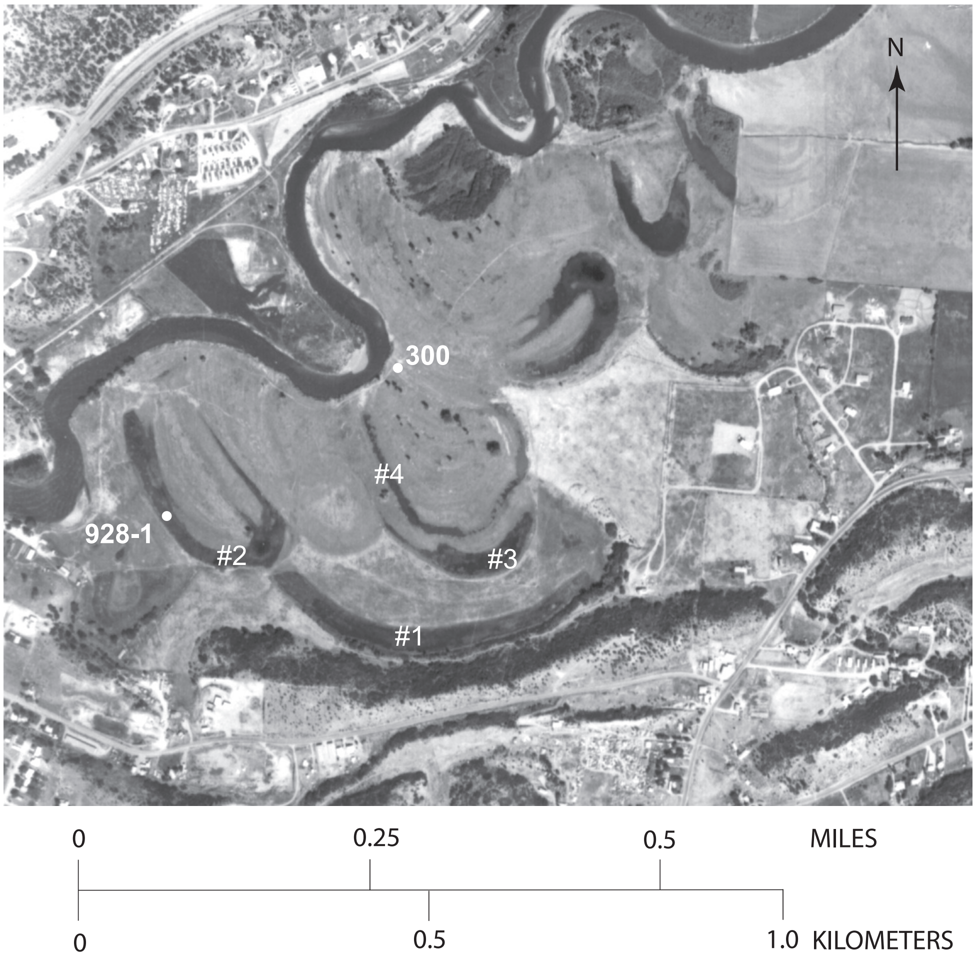

Figure 2. Enlargement of the 1973 aerial photograph showing the active meander of the Animas River and oxbow lakes sampled just north of Durango, Colo. Downstream is to the left; north is at the top of the photograph. Core localities are shown for samples taken for flux determinations (tables 1 and 2). Oxbow lakes are numbered in the order they formed: oxbow lake #1 is the oldest, oxbow lake #4 (core 97ABS300; 300 on figure) the youngest. Oxbow lake #4 was active when the initial topographic mapping was completed in 1896 (U.S. Geological Survey, 1898). Core locality for dated core (99928; 928-1 on figure) shown in oxbow lake #2. .

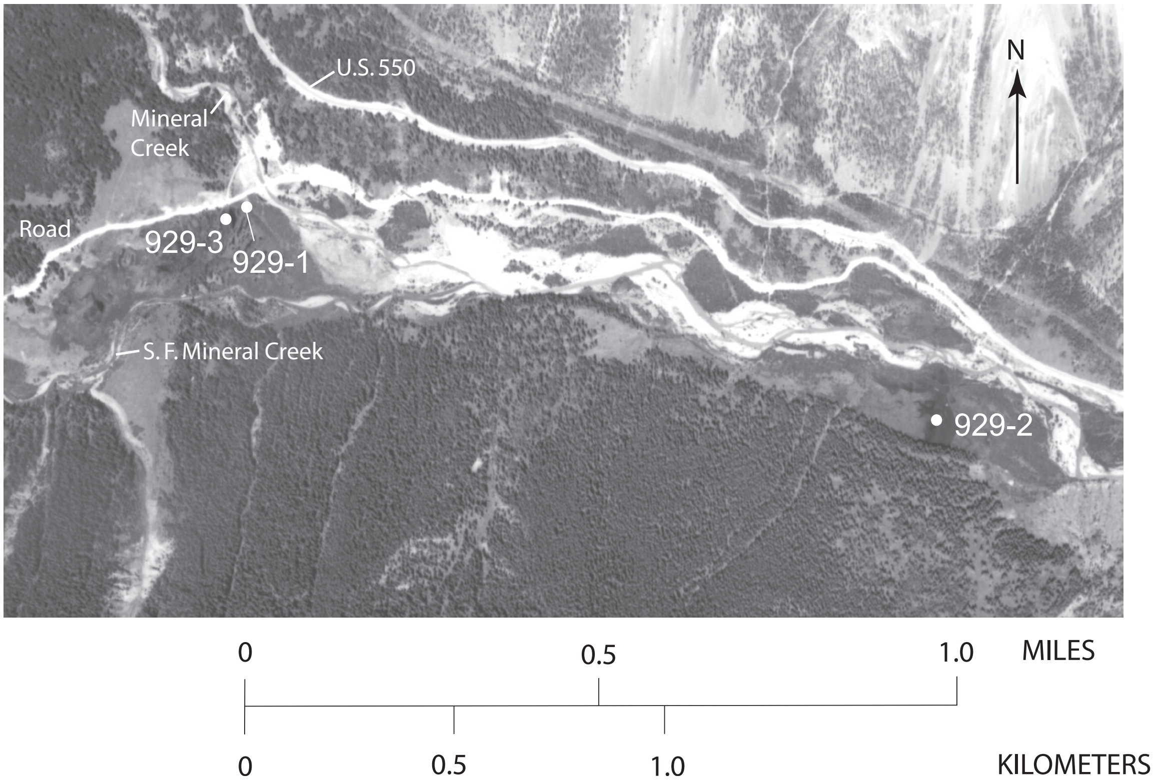

Figure 3. Enlargement of the 1973 aerial photograph taken near the confluence of Mineral Creek with the South Fork Mineral Creek showing localities of abandoned beaver ponds sampled west of Silverton, Colo. Downstream is to the right; north is at the top of the photograph. Elevations of both sets of beaver ponds are above flood stage, and the ponds are ground-water fed. Sultan Mountain, composed largely of unmineralized granodiorite, is south of site 929-2, and peak 3,792 m, underlain by a porphyry copper-molybdenum deposit, is northwest of site 929-3. Core numbers have been abbreviated on figure.

Methods of Study

Depositional Site Characteristics

Samples for this study were collected from two different depositional environments, both of which are geomorphologically distinct. Many stream reaches in the headwaters are downcutting, have broad to narrow riparian zones (fig. 3), and often support an active beaver population. Beaver ponds in the upper watershed in the Mineral Creek drainage basin are built on the sides of the riparian zone, trapping ground water before it enters the streams. The downstream reach of the Animas River has numerous meanders and has created many generations of oxbow lakes (fig. 2). The depositional environments of beaver ponds and oxbow lakes provide ideal sedimentary repositories that preserve a stratigraphic and chronologic record of environmental change in the watershed, and both depositional environments have low sedimentation rates and significant spring-fed ground-water components in their water budgets (Fey and others, 2000). In this study, we report the results of geochemical, lead (Pb) isotopic, and radionuclide data from these young sediment catchments to document the recent changes (<200 yr) in geochemistry caused by historical mining.

Sample Collection

Sediment Cores

Sediment cores were collected by driving and subsequently extracting sections of 10-cm-diameter PVC pipe that had previously been acid-cleaned and water-rinsed into the sediment (sites 99928-1; 99929-1 through 99929-3). These cores were subsequently split lengthwise and sampled in 1–2 cm intervals, taking care to avoid material in contact with the core liner and along the split-core surface, to give the time resolution needed for the study. Core 97ABS300 was a 5-cm-diameter core that was subdivided based on stratigraphic, color, and grain-size differences (Fey and others, 2000). Core sample localities and depth intervals are in table 1. Subsamples from the cores were subsequently analyzed for radionuclides, element abundances, and loss-on-ignition.

Table 1. Sample localities and data on cores, Animas River watershed, Colorado.
[Core 97ABS300 collected by D.L. Fey and S.E. Church, property accessed by permission; other cores collected by C.W. Holmes, M.E. Marot, and S.E. Church on USDA Forest Service land. DD, decimal degrees]

Core no.	Date collected	Latitude DD	Longitude DD	Diameter of core (cm)	Total depth (cm)
99928-1	28-Sep-99	37.29992	107.85964	10	42
97ABS300	16-Aug-97	37.30483	107.85519	5	238
99929-1	29-Sep-99	37.81767	107.72000	10	54
99929-2	29-Sep-99	37.81553	107.70283	10	46
99929-3	29-Sep-99	37.81786	107.72039	10	65

Sample Preparation

Core subsamples were air dried. The midpoint of the depth interval for each subsample is used as the depth for that subsample. No depth corrections for compression were made on the 10-cm-diameter cores. Samples with high organic content (peat) were ashed prior to analysis (Fey and others, 2000).

Because the grain size in all samples except those from core 97ABS300 was predominately silt, subsamples were mixed but not ground to finer grain size. Core 97ABS300 was expanded linearly to correct for compression (Fey and others, 2000). Core compaction was determined by measuring the depth of penetration of the core casing in the field, and then measuring the length of the recovered core material. Subsamples from core 97ABS300 were air dried, sieved if the grain size exceeded that of fine sand (0.125–0.25 mm), and the fines retained and ground in random order to minus 100 mesh in a vertical pulverizer. The grain size and sample type are briefly described for each interval in the data tables (2–6). The peat zones in the beaver ponds are described in tables 4–6 as matted fiber or grass.

Analytical Methods and Results

Geochemical Analyses

Trace-Element Analysis by Inductively Coupled Plasma–Atomic Emission Spectrometry

The samples were digested with a mixed-acid procedure consisting of hydrochloric, nitric, perchloric, and hydrofluoric acids (HCl, HNO_3, $HClO_4$, and HF) (Crock and others, 1983; Briggs, 2002). This procedure is effective in dissolving most minerals, including silicates, oxides and sulfides; resistant or refractory minerals such as zircon, chromite, and some tin oxides are only partially dissolved. Previous investigations using a variety of materials support the completeness of the digestion (Church, 1981; Church and others, 1987; Wilson and others, 1994). Trace- and major-element data (tables 2–6) were determined by ICP–AES (inductively coupled plasma–atomic emission spectrometry; Briggs, 2002). ICP–AES data are reported for As, Cd, Cu, Pb, Mn, Ag, and Zn for all sample intervals, and for the major elements if the core subsample was not analyzed by X-ray fluorescence (Fey and others, 2000). Limits of determination for the ICP–AES total digestion multi-acid method as well as a statistical summary of mean values, standard deviations, and median values for four National Institute of Standards and Technology (NIST) standard reference materials (SRM-2704, SRM-2709, SRM-2710, and SRM-2711) are given in Fey and others (1999). In addition, comparisons with certified values for these standards (NIST, 1993a,b,c,d) are in Fey and others (1999). Both analytical precision and accuracy are well within acceptable ranges of error for the method (Briggs, 2002).

X-Ray Fluorescence Analysis

Samples from cores 99928-1 (table 2), 99929-2 (table 5), and 97ABS300 (table 3) were also analyzed using wavelength-dispersive X-ray fluorescence spectrometry (Taggart and others, 1987) by a contract laboratory to obtain more reliable and accurate major-element data including SiO_2. X-ray fluorescence data for SiO_2 were found to be important to track the contribution of windblown mill tailings to sediment in the two small catchment basins (cores 99928-1 and 99929-2) because the ore milled at the Sunnyside Mill at Eureka during the period from 1900–1915 was predominately galena in quartz (SiO_2) veins (Jones, 2007). SiO_2 is an important sedimentological and geochemical marker used in conjunction with Pb concentrations to determine the 1911 flood event recorded in core 97ABS300.

Table 2. Core descriptions, depths, and geochemical data from core 99928-1.

[Core descriptions from Fey and others (2000), table 5; ICP–AES data from table 9; x-ray fluorescence data by contract laboratory]

			X-ray fluorescence data										ICP–AES data						
Field sample no.	Sample interval midpoint depth (cm)	Subinterval sample description	Al_2O_3 wt. %	CaO wt. %	Fe_2O_3 wt. %	K_2O wt. %	MgO wt. %	MnO wt. %	Na_2O wt. %	P_2O_5 wt. %	SiO_2 wt.%	TiO_2 wt. %	Arsenic ppm	Cadmium ppm	Copper ppm	Lead ppm	Manganese ppm	Silver ppm	Zinc ppm
999281-1	1	light-brown silt, some grass fibers	17.42	2.23	7.73	3.81	2.58	0.56	1.24	0.38	63.20	0.83	31	10	360	1,400	2,800	8	2,200
999281-2	2	light-brown silt, twigs, root mat	17.46	1.69	7.21	3.70	2.54	0.44	1.29	0.34	64.51	0.83	32	8	360	1,500	2,400	9	2,100
999281-3	3	light-brown silt, twigs, root mat	17.53	1.52	7.36	3.71	2.50	0.58	1.25	0.33	64.41	0.82	27	9	510	2,000	3,400	11	2,400
999281-4	4	light-brown silt, twiglets	17.62	1.49	7.28	3.73	2.47	0.55	1.27	0.32	64.46	0.81	30	9	460	1,800	3,100	10	2,100
999281-5	5	light-brown silt, rootlets	17.48	1.51	7.58	3.71	2.52	0.Z39	1.32	0.30	64.34	0.84	36	9	360	1,500	2,300	8	2,000
999281-6	6	light-brown silt, rootlets	17.42	1.58	7.63	3.71	2.53	0.36	1.35	0.30	64.29	0.82	30	8	320	1,300	2,100	7	1,800
999281-7	7	light-brown silt, rootlets	17.58	1.63	7.59	3.72	2.57	0.34	1.37	0.31	64.07	0.82	33	8	310	1,300	2,100	7	1,800
999281-8	8	light-brown silt, rootlets	17.30	1.55	7.57	3.69	2.52	0.32	1.34	0.29	64.58	0.83	26	8	310	1,200	1,900	6	1,700
999281-9	9	light-brown silt, sparse fibers	16.91	1.51	7.78	3.63	2.44	0.32	1.38	0.28	64.95	0.81	28	7	300	1,200	2,000	7	1,800
999281-10	10	light-brown silt, sparse fibers	16.65	1.50	7.76	3.55	2.40	0.37	1.40	0.27	65.30	0.79	34	8	360	1,500	2,500	8	2,100
999281-12	11	light-brown silt, sparse fibers	16.61	1.50	7.61	3.54	2.42	0.38	1.42	0.27	65.42	0.82	33	8	340	1,300	2,400	7	1,800
999281-14	13	light-brown silt, sparse fibers	15.86	1.43	7.39	3.42	2.33	0.32	1.54	0.24	66.69	0.79	27	5	150	430	2,100	2	990
999281-16	15	light-brown silt, sparse fibers	14.37	1.37	6.82	3.18	2.07	0.24	1.70	0.23	69.26	0.76	20	4	64	140	1,700	<2	520
999281-18	17	light-brown silt, sparse fibers	14.36	1.77	6.88	3.16	2.20	0.31	1.64	0.23	68.68	0.78	21	3	63	270	2,100	<2	480
999281-20	19	light-brown silt, sparse fibers	14.44	3.63	6.98	3.09	2.28	0.35	1.56	0.23	66.65	0.79	13	3	59	94	2,300	<2	380
999281-22	21	light-brown silt and clay, blocky	14.18	4.20	6.95	3.05	2.25	0.32	1.59	0.22	66.47	0.78	16	3	47	63	2,100	<2	270
999281-24	23	light-brown silt and clay, blocky, sparse fibers	13.80	4.49	6.59	2.98	2.22	0.28	1.59	0.21	67.07	0.76	21	2	43	58	1,900	<2	250
999281-26	25	light-brown silt and clay, blocky, sparse fibers	13.20	3.26	5.94	2.97	2.07	0.24	1.74	0.19	69.69	0.71	18	2	44	53	1,700	<2	200
999281-28	27	light-brown silt, no clay	12.85	3.10	5.50	2.96	1.91	0.19	1.85	0.18	70.82	0.64	14	2	33	48	1,500	<2	180
999281-30	29	silt and clay, blocky	13.21	3.84	6.01	2.97	2.07	0.19	1.76	0.19	69.07	0.68	14	2	42	52	1,400	<2	200
999281-32	31	silt and clay, blocky	13.58	4.06	6.33	3.00	2.20	0.19	1.65	0.21	68.06	0.74	15	2	47	47	1,200	<2	200
999281-34	33	silt and clay, blocky	13.59	2.89	6.19	3.04	2.09	0.18	1.81	0.19	69.32	0.70	17	2	39	50	1,300	<2	200
999281-36	35	silt and clay, blocky	13.41	1.74	5.83	3.08	1.92	0.16	1.91	0.17	71.15	0.63	16	2	40	57	1,200	<2	200
999281-38	37	fine sand and silt	13.04	1.33	5.22	3.10	1.73	0.15	2.02	0.15	72.71	0.56	16	2	75	52	1,100	<2	200
999281-40	39	fine sand and silt	13.02	1.38	5.34	3.05	1.77	0.17	2.01	0.17	72.51	0.59	13	2	39	52	1,300	<2	180
999281-42	41	fine sand and silt	13.03	1.42	5.34	3.05	1.78	0.16	1.95	0.18	72.48	0.61	19	2	41	52	1,300	<2	180

Table 3. Core descriptions, depths, and geochemical data from core 97ABS300.

[Core descriptions from Fey and others (2000), table 5; ICP–AES data from table 9; sulfur and x-ray fluorescence data by contract laboratory]

				X-ray fluorescence data										ICP–AES data						
Field sample no.	Sample interval midpoint depth (cm)	Subinterval sample description	Sulfur wt. %	Al_2O_3 wt. %	CaO wt.%	Fe_2O_3 wt.%	K_2O wt. %	MgO wt. %	MnO wt.%	Na_2O wt. %	P_2O_5 wt. %	SiO_2 wt. %	TiO_2 wt. %	Arsenic ppm	Cadmium ppm	Copper ppm	Lead ppm	Manganese ppm	Silver ppm	Zinc ppm
97ABS300A-a2	6	medium-brown silt, micaceous, soil, grass roots	0.12	11.43	1.87	4.55	2.76	1.50	0.78	1.40	0.18	74.92	0.61	28	8	270	700	5,500	6	1,700
97ABS300A-b2	21	dark-brown fine sand and silt, roots	1.44	10.30	3.74	3.51	2.29	1.18	2.42	0.88	0.19	74.96	0.52	25	22	300	980	14,000	10	3,200
97ABS300A-c2	47	medium-brown fine sand and silt, mica, minor iron-oxide staining	0.41	9.44	2.12	3.76	1.95	1.04	2.93	0.94	0.18	77.19	0.44	34	4	450	2,800	19,000	21	700
97ABS300A-d2	59	medium-brown and tan silt and clay, fine sand, minor orange iron-oxidation staining, few root twigs	0.77	9.95	2.30	3.23	2.06	1.10	2.88	1.07	0.15	76.85	0.42	25	6	530	1,300	18,000	14	1,100
97ABS300A-e1	67	tan fine sand and silt, moderate iron-oxide staining, some root twigs	0.44	8.72	2.06	3.43	1.78	0.97	3.03	0.89	0.16	78.57	0.39	29	3	350	2,200	19,000	19	650
97ABS300A-f1	74	tan and buff fine sand	1.39	7.64	2.86	2.96	1.38	0.79	4.19	0.63	0.15	79.07	0.34	35	3	500	2,900	24,000	25	690
97ABS300A-g1	77	dark and tan fine sand, one 1-cm-diameter root fragment	1.40	9.28	2.53	2.95	1.77	0.90	4.51	0.92	0.15	76.59	0.40	29	6	650	1,700	24,000	19	1,100
97ABS300A-h1	81	dark and tan fine sand, a few 2-mm root twigs, possible clay in sample	1.05	9.88	2.49	3.26	1.95	1.08	3.69	0.98	0.16	76.05	0.46	28	7	500	1,700	22,000	18	1,200
97ABS300A-i3	93	light-tan fine sand and silt, no rootlets	1.64	9.45	2.98	2.81	1.74	1.00	4.72	0.77	0.16	75.98	0.40	29	7	530	2,000	26,000	19	1,700
97ABS300A-j1	112	medium-brown fine sand, a little orange staining, sparse rootlets	0.84	9.39	2.39	2.45	1.77	0.96	4.51	0.89	0.16	77.07	0.41	26	10	510	1,900	26,000	19	1,300
97ABS300A-k3	126	orange-buff silt, strong iron-oxide staining, root twig to 8-mm diameter	0.54	8.02	2.70	2.53	1.40	0.81	4.77	0.58	0.15	78.71	0.33	33	3	540	2,800	27,000	26	850
97ABS300A-k5	133	orange-buff silt	1.13	7.33	4.32	2.00	1.22	0.70	5.38	0.44	0.14	78.17	0.29	37	4	630	4,400	28,000	32	770
97ABS300A-m1	141	buff-tan and darker, fine sand and silt, little iron-oxidation, mica	0.80	8.63	2.15	2.57	1.75	0.86	3.42	0.94	0.14	79.17	0.37	26	8	600	1,600	23,000	16	1,100
97ABS300A-n2	154	buff-tan fine sand and silt, a few small twigs	1.03	9.24	2.45	2.58	1.85	0.98	3.59	0.91	0.14	77.88	0.39	26	8	470	1,300	21,000	14	1,100
97ABS300A-o2	181	dark gray-brown silt, mafics, some root fibers	0.07	11.57	1.47	3.77	2.51	1.34	2.35	1.40	0.18	74.87	0.54	23	8	440	1,100	15,000	10	1,200
97ABS300A-p2	194	gray-brown fine sand, sparse root fibers and twigs	0.14	10.57	1.32	3.42	2.43	1.09	1.61	1.62	0.15	77.30	0.48	17	6	310	590	11,000	7	890
97ABS300A-q2	218	medium-brown fine sand and silt, micaceous, minor iron-oxide staining, a few root fibers	0.07	10.40	1.44	3.55	2.41	1.12	1.44	1.55	0.15	77.44	0.50	20	9	340	580	10,000	8	2,000
97ABS300A-r2	231	tan-gray silt, some scattered iron-oxide staining	0.10	11.62	1.85	4.12	2.61	1.55	1.38	1.29	0.19	74.81	0.59	26	13	410	1,200	9,000	8	3,700

Table 4. Core descriptions, depths, and geochemical data from core 99929-1.

[Core descriptions from Fey and others (2000), table 2; ICP–AES data from table 6]

			ICP–AES data													
Field sample no.	Sample interval midpoint depth (cm)	Subinterval sample description	Aluminum wt. %	Calcium wt. %	Magnesium wt. %	Iron wt. %	Sodium wt. %	Potassium wt. %	Titanium wt. %	Arsenic ppm	Cadmium ppm	Copper ppm	Lead ppm	Manganese ppm	Silver ppm	Zinc ppm
999291-1	1	light-brown silt	2.8	0.09	0.23	30	0.26	0.63	0.09	14	8	10	8	68	<2	39
999291-2	2	light-brown silt	4.2	0.14	0.31	20	0.34	0.82	0.12	<10	5	19	6	98	<2	42
999291-3	3	light-brown silt	3.0	0.15	0.24	30	0.24	0.61	0.09	<10	9	4	9	71	<2	30
999291-4	4	light-brown silt	3.2	0.19	0.26	30	0.25	0.66	0.09	13	9	6	6	80	<2	26
999291-5	5	light-brown silt, some orange coloration	4.8	0.23	0.35	25	0.37	0.96	0.11	16	8	32	13	130	<2	33
999291-6	6	light-brown silt, some orange coloration	6.0	0.20	0.47	21	0.41	1.30	0.14	16	6	13	24	180	<2	39
999291-7	7	light-brown silt, some orange coloration	5.3	0.18	0.42	25	0.34	1.10	0.13	12	8	11	20	140	<2	48
999291-8	8	light-brown silt, some orange coloration	3.4	0.13	0.24	34	0.21	0.64	0.09	11	9	4	9	59	<2	36
999291-9	9	light-brown silt, some orange coloration	2.3	0.09	0.12	41	0.12	0.32	0.06	<10	11	<1	<4	5	<2	27
999291-10	10	light-brown silt, some orange coloration	2.2	0.08	0.10	38	0.10	0.27	0.05	<10	10	3	<4	4	<2	25
999291-12	12	light-brown silt, some orange coloration	2.2	0.08	0.11	39	0.10	0.26	0.05	<10	10	8	<4	<4	<2	33
999291-14	14	light-brown silt, some orange coloration	2.5	0.10	0.12	36	0.12	0.30	0.05	<10	9	<1	<4	9	<2	44
999291-16	16	light-brown silt, some orange coloration	2.8	0.11	0.13	36	0.12	0.31	0.06	<10	10	9	<4	12	<2	54
999291-18	18	light-brown silt, less orange	2.4	0.13	0.13	32	0.13	0.33	0.06	<10	8	12	<4	15	<2	62
999291-20	20	brown silt	3.3	0.08	0.07	38	0.05	0.14	0.03	<10	9	<1	<4	<4	<2	68
999291-22	22	brown silt	3.3	0.11	0.09	36	0.07	0.18	0.04	<10	10	7	<4	<4	<2	27
999291-24	24	brown with orange silt	3.3	0.06	0.06	39	0.04	0.11	0.03	<10	10	8	<4	<4	<2	86
999291-26	26	brown and orange silt, iron-oxide clumps	3.2	0.03	0.05	40	0.04	0.10	0.03	<10	10	1	<4	<4	<2	52
999291-28	28	orange-brown silt with some plant fibers	4.1	0.02	0.04	39	0.02	0.06	0.02	<10	11	3	<4	<4	<2	49
999291-30	30	orange-brown silt with some plant fibers	4.9	0.02	0.04	35	0.03	0.08	0.02	<10	10	9	<4	<4	<2	61
999291-32	32	tan-brown silt	5.0	0.03	0.08	27	0.07	0.17	0.04	29	8	<1	<4	<4	<2	48
999291-34	34	orange-brown silt with grass fibers	5.0	0.02	0.06	27	0.05	0.13	0.03	<10	8	7	<4	<4	<2	40
999291-36	36	brown-orange silt with grass fibers	5.5	0.02	0.05	27	0.04	0.11	0.03	<10	7	<1	<4	<4	<2	28
999291-38	38	brown-orange silt with grass fibers	5.8	0.03	0.08	22	0.08	0.19	0.04	<10	7	6	<4	6	<2	30
999291-40	40	tan-brown silt	5.8	0.05	0.09	20	0.10	0.22	0.05	<10	6	1	<4	9	<2	40
999291-42	42	brown-gray silt and matted fibers	5.8	0.06	0.10	17	0.11	0.23	0.05	10	5	4	<4	14	<2	36
999291-44	44	gray-brown silt	5.3	0.07	0.11	12	0.13	0.26	0.06	<10	3	13	<4	19	<2	36
999291-46	46	gray-brown silt	4.2	0.07	0.10	8.4	0.10	0.23	0.05	< 10	3	10	< 4	25	< 2	29
999291-48	48	gray-brown silt	3.9	0.07	0.10	6.6	0.11	0.23	0.04	< 10	3	12	< 4	22	< 2	26
999291-50	50	matted fibers	4.3	0.08	0.12	5.3	0.12	0.25	0.04	< 10	3	12	5	33	< 2	31
999291-52	52	fine mix of fiber and silt	4.3	0.10	0.12	5.1	0.13	0.26	0.04	< 10	3	12	4	33	< 2	39
999291-54	54	fine mix of fiber and silt	4.3	0.09	0.15	8.9	0.16	0.38	0.06	< 10	3	13	5	40	< 2	38

Table 5. Core descriptions, depths, and geochemical data from core 99929-2.

[Core descriptions from Fey and others (2000), table 2; ICP–AES data from table 6; sulfur and x-ray fluorescence data by contract laboratory; --, no data]

				X-ray fluorescence data										ICP–AES data						
Field sample no.	Sample interval midpoint depth (cm)	Subinterval sample description	Sulfur wt. %	Al_2O_3 wt. %	CaO wt. %	Fe_2O_3 wt. %	K_2O wt. %	MgO wt. %	MnO wt. %	Na_2O wt. %	P_2O_5 wt. %	SiO_2 wt. %	TiO_2 wt. %	Arsenic ppm	Cadmium ppm	Copper ppm	Lead ppm	Manganese ppm	Silver ppm	Zinc ppm
999292-2	2	tan-gray silt, one root twig discarded	4.42	9.07	1.56	13.18	1.91	1.15	0.03	0.41	0.73	71.56	0.41	30	9	150	210	170	<2	2,200
999292-3	3	tan-gray silt	6.43	9.18	1.74	14.87	1.85	1.15	0.04	0.42	0.58	69.76	0.41	31	10	160	210	200	<2	2,600
999292-4	4	tan-gray silt	7.62	10.25	2.07	15.66	1.97	1.22	0.06	0.53	0.46	67.34	0.44	38	9	200	240	240	<2	2,200
999292-5	5	tan-gray silt	8.28	11.62	2.06	16.44	2.15	1.30	0.06	0.57	0.44	64.88	0.48	57	10	260	280	260	<2	2,200
999292-6	6	tan-gray silt	9.30	13.60	2.18	18.35	2.38	1.39	0.06	0.64	0.61	60.25	0.54	55	9	330	310	290	<2	2,100
999292-7	7	tan-gray silt	11.05	12.54	2.48	22.61	2.35	1.50	0.09	0.67	0.48	56.75	0.54	49	9	210	250	340	<2	1,800
999292-8	8	tan-gray silt	--	--	--	--	--	--	--	--	--	--	--	42	8	130	270	300	<2	1,500
999292-9	9	tan-gray silt	9.26	13.39	3.40	21.56	2.77	1.74	0.06	0.88	0.37	55.16	0.68	34	7	140	350	240	<2	1,400
999292-10	10	tan-gray silt with some plant fibers	9.56	13.31	3.53	22.78	2.75	1.73	0.07	0.89	0.38	53.89	0.66	48	7	140	350	230	<2	1,400
999292-12	12	tan-gray silt	7.64	15.07	3.70	20.45	3.13	1.94	0.07	0.98	0.44	53.46	0.77	50	7	120	500	220	<2	1,600
999292-14	14	matted fiber	--	18.04	2.81	10.39	3.50	2.14	0.06	1.34	0.38	60.55	0.80	36	5	120	700	290	2	950
999292-16	16	matted fiber	--	22.99	2.92	5.60	2.78	1.86	0.06	1.39	0.28	61.33	0.79	26	4	97	540	240	<2	910
999292-18	18	matted fiber	--	14.97	3.52	5.93	2.87	1.70	0.04	1.67	0.34	68.12	0.83	18	3	54	270	230	<2	740
999292-20	20	matted fiber	--	14.79	4.23	5.73	2.81	1.74	0.04	1.69	0.43	67.71	0.83	15	<2	36	99	190	<2	200
999292-22	22	matted fiber	--	14.98	4.15	5.53	2.84	1.75	0.04	1.72	0.42	67.72	0.84	12	<2	32	97	200	<2	170
999292-24	24	silt and fine fiber	--	15.00	3.88	5.61	2.89	1.77	0.04	1.75	0.39	67.83	0.84	15	<2	39	140	220	<2	220
999292-26	26	gray-brown silt and mats	--	14.77	4.07	6.38	2.82	1.73	0.04	1.69	0.43	67.22	0.83	14	<2	34	120	210	<2	210
999292-28	28	gray-brown silt and mats	--	14.26	5.14	9.68	2.71	1.72	0.05	1.54	0.48	63.61	0.81	10	<2	30	63	160	<2	170
999292-30	30	clumps of matted fiber and silt	--	12.72	4.83	18.39	2.37	1.57	0.05	1.34	0.53	57.46	0.74	18	2	25	39	130	<2	250
999292-32	32	gray silt	--	15.36	3.37	9.01	2.82	1.92	0.06	1.69	0.40	64.50	0.87	16	2	35	60	260	<2	240
999292-34	34	gray and tan clumps of silt and fiber	--	16.21	2.83	10.38	2.90	2.08	0.06	1.61	0.37	62.71	0.87	20	3	40	78	300	<2	200
999292-36	36	tan-brown silt, little fiber	2.16	16.78	2.80	9.65	3.06	2.10	0.07	1.56	0.34	62.74	0.90	24	3	46	87	320	<2	220
999292-38	38	gray-brown clumps of clay and silt and fiber	--	18.53	3.11	7.84	3.25	2.26	0.06	1.41	0.47	62.33	0.75	12	3	54	78	270	<2	230
999292-40	40	medium-brown material	--	17.55	10.40	13.98	2.84	2.08	0.04	0.90	1.18	50.39	0.64	<10	<2	70	23	74	<2	96
999292-42	42	medium-brown material	--	13.89	14.07	17.62	2.34	1.70	0.03	0.84	1.08	47.80	0.63	<10	3	43	11	39	<2	420
999292-44	44	medium-brown material	--	13.30	8.81	31.94	2.51	1.79	0.05	0.86	0.69	39.42	0.63	11	4	32	30	92	<2	490
999292-46	46	medium-brown material	--	13.47	6.07	22.59	2.47	1.65	0.05	0.99	0.66	51.42	0.64	19	4	69	120	130	<2	570

Table 6. Core descriptions, depths, and geochemical data from core 99929-3.

[Core descriptions from Fey and others (2000), table 2; ICP–AES data from table 6]

Field sample no.	Sample interval midpoint depth (cm)	Subinterval sample description	ICP–AES data													
			Aluminum wt. %	Calcium wt. %	Magnesium wt. %	Iron wt. %	Sodium wt. %	Potassium wt. %	Titanium wt. %	Arsenic ppm	Cadmium ppm	Copper ppm	Lead ppm	Manganese ppm	Silver ppm	Zinc ppm
999293-2	2	orange clayey silt	3.8	0.09	0.34	24.0	0.34	0.86	0.10	15	6	21	15	120	<2	51
999293-3	3	orange clayey silt	5.0	0.11	0.42	21.0	0.48	1.20	0.14	16	7	20	22	160	<2	44
999293-4	4	orange clayey silt	7.0	0.14	0.56	13.0	0.60	1.60	0.16	14	4	29	38	220	<2	43
999293-5	5	tan-brown clayey silt	7.6	0.22	0.69	5.3	0.80	1.80	0.19	<10	2	28	53	320	<2	54
999293-6	6	orange-brown clayey silt	6.0	0.19	0.47	15.0	0.56	1.30	0.16	22	4	20	30	190	<2	78
999293-7	7	tan-brown clayey silt	5.0	0.16	0.63	6.9	0.73	1.20	0.19	16	2	22	28	310	<2	86
999293-8	8	tan-brown clayey silt	4.5	0.16	0.42	5.9	0.43	1.10	0.16	10	2	26	23	130	<2	48
999293-9	9	tan-orange clayey silt	4.5	0.15	0.42	10.0	0.42	1.10	0.16	15	3	20	21	120	<2	66
999293-10	10	orange silt	3.6	0.14	0.40	19.0	0.39	0.99	0.14	<10	5	32	18	110	<2	39
999293-12	12	orange silt	2.2	0.09	0.23	29.0	0.24	0.61	0.10	<10	8	8	<4	48	<2	28
999293-14	14	orange silt	2.5	0.12	0.25	20.0	0.28	0.71	0.12	<10	5	11	<4	48	<2	20
999293-16	16	tan silt	2.9	0.14	0.28	5.5	0.37	0.92	0.15	<10	<2	17	7	56	<2	16
999293-18	18	tan silt	2.6	0.12	0.24	3.5	0.33	0.82	0.14	<10	<2	12	6	49	<2	13
999293-20	20	light-tan silt	2.2	0.11	0.20	3.0	0.29	0.68	0.11	<10	<2	12	4	42	<2	12
999293-22	22	tan-gray silt	2.6	0.14	0.21	3.0	0.34	0.83	0.14	<10	<2	19	8	45	<2	14
999293-24	24	light-brown silt	3.0	0.20	0.23	5.9	0.25	0.75	0.14	<10	2	16	6	51	<2	40
999293-26	26	light-brown silt, some fibrous material	2.7	0.23	0.19	5.7	0.19	0.59	0.13	<10	2	14	5	56	<2	81
999293-28	28	medium-brown silt	2.5	0.25	0.17	4.8	0.18	0.51	0.10	<10	2	13	5	56	<2	120
999293-30	30	medium-brown silt and fiber	2.3	0.24	0.14	6.7	0.14	0.39	0.08	21	3	16	14	58	<2	100
999293-32	32	medium-brown silt and fiber	3.0	0.37	0.20	6.1	0.29	0.60	0.10	20	3	17	18	93	<2	160
999293-34	34	medium-brown silt and much fiber	3.9	0.44	0.25	13.0	0.31	0.70	0.12	44	6	21	24	130	<2	370
999293-36	36	brown silt	2.7	0.26	0.15	14.0	0.20	0.44	0.08	32	4	16	16	97	<2	170
999293-38	38	blocky silt, clay and fibrous clumps	5.0	0.50	0.32	6.2	0.50	0.93	0.15	18	3	24	26	150	<2	120
999293-40	40	medium-brown silt and fine organic fibers	4.9	0.29	0.14	2.7	0.15	0.35	0.06	15	<2	31	24	51	<2	92
999293-42	42	mostly pressed fiber	4.4	0.24	0.08	2.2	0.08	0.19	0.04	<10	<2	20	13	35	<2	70
999293-44	44	mostly pressed fiber	3.3	0.18	0.07	9.3	0.06	0.15	0.03	<10	4	9	6	40	<2	54
999293-46	46	mostly pressed fiber	3.9	0.17	0.10	6.6	0.06	0.21	0.04	<10	2	10	4	35	<2	33
999293-48	48	mostly pressed fiber	4.6	0.18	0.09	3.5	0.07	0.20	0.04	<10	2	13	6	31	<2	54
999293-50	50	mostly pressed fiber	3.5	0.14	0.07	7.6	0.08	0.19	0.04	<10	3	11	<4	36	<2	51
999293-52	52	mostly pressed fiber	2.3	0.09	0.06	4.1	0.07	0.18	0.03	<10	<2	4	<4	26	<2	32
999293-54	54	mostly pressed fiber	3.3	0.14	0.08	9.0	0.10	0.23	0.04	<10	3	7	<4	39	<2	36
999293-56	56	mostly pressed fiber	3.6	0.13	0.10	6.6	0.07	0.24	0.04	<10	3	12	<4	36	<2	44
999293-58	58	mostly pressed fiber	3.4	0.13	0.09	7.8	0.09	0.24	0.04	<10	3	13	<4	34	<2	46
999293-60	60	mostly pressed fiber	3.8	0.15	0.13	5.5	0.15	0.34	0.06	<10	2	15	7	45	<2	58
999293-62	62	mostly pressed fiber	4.2	0.15	0.18	4.4	0.18	0.46	0.08	10	<2	14	13	56	<2	81
999293-65	65	mostly pressed fiber	4.3	0.21	0.22	4.0	0.24	0.54	0.10	<10	<2	25	21	75	<2	72

Radionuclide Analysis

^{210}Pb activity was measured by alpha spectroscopy. The ^{210}Pb (half-life = 22.3 yr) alpha method is based on determining the activity of polonium-210 (^{210}Po), which is assumed to be in secular equilibrium with its parent ^{210}Pb. The analytical method exploits the ability of polonium to auto-plate onto silver planchets, which facilitates the alpha counting (Flynn, 1968). Briefly, 5 g of sediment was hand-ground in a mortar and pestle and fired in a muffle furnace at 550°C for 6 hours to determine loss-on-ignition (LOI). The percent ash content (determined from the LOI) of samples containing organic matter (peat) is provided for samples that were ashed prior to analysis. The fired material was transferred to a glass beaker, ^{210}Po was acid-leached from the sediment, and a known quantity of the tracer ^{209}Po was added to the solution prior to auto-plating the polonium isotopes onto silver planchets. The planchets were counted in low-level alpha spectrometers coupled to a pulse-height analyzer.

Gamma spectroscopy was used to determine the beryllium-7 (^{7}Be) (half-life = 53 d), cesium-137 (^{137}Cs) (half-life = 30.2 yr), and radium-226 (^{226}Ra) (half-life = 1,600 yr) activities in each sample (Cutshall and others, 1983). A 50-g aliquot of dried and ground sample was sealed in a plastic counting jar. Sealed samples were stored for at least 20 days to allow ^{222}Ra and ^{214}Pb activity to come into equilibrium with their parent isotope (^{226}Ra). Samples were counted by a germanium detector (2,000-mm^2 area) for low-energy gamma rays, and data were collected using a 4,096 channel multi-channel analyzer. Samples were typically counted for 24 hours (depending on sample size) or until counting errors were less than 5 percent. The gamma system was calibrated using a NIST-traceable multi-line radioisotope standard in a soil matrix with the same counting geometry as the samples. Specific activity of ^{226}Ra was determined from counts associated with the photo-peaks of ^{214}Pb (295 and 351 kev) and ^{214}Bi (bismuth-214) (609 kev). Activities calculated from the three peaks were combined to yield a weighted-mean reported value and standard deviation. The gamma-ray counting system was calibrated and frequently checked by counting radioisotope standards prepared by doping portions of Florida Bay sediment with precisely known amounts of a radium standard solution (Robbins and others, 2000). This solution has a 0.4 percent uncertainty in activity at the 99 percent confidence level, which is due to random counting errors, and an additional 0.8 percent uncertainty due to assessable systematic counting errors. Reported standard deviations in ^{226}Ra activity, including random errors associated with detector calibration, were typically 5–7 percent. The limit of detection was about 0.1 dpm/g (disintegrations per minute/gram) for this sample matrix. ^{7}Be and ^{137}Cs activities were determined by counting the 477 kev and 661.6 kev gamma ray peaks, respectively. All activities were decay corrected to the date of sample collection. The reported errors are the statistical counting errors at the 95 percent confidence interval. Total analytical errors are about ±6.5 percent based on replicate sample analyses. Analytical data are reported in tables 7–10.

Calculations of the ^{210}Pb and ^{137}Cs flux (dpm/cm^2/yr) and inventories (dpm/cm^2) are also included in tables 7–10. The inventory of ^{210}Pb was determined over the last 150 yr in the dated portions of the cores and the flux estimated as that required to produce the observed inventory when corrected for decay. For ^{137}Cs, the inventory is the sum over intervals where ^{137}Cs was detected, and the flux is the inventory divided by the number of years during which ^{137}Cs was observed.

Table 7. Sample depths, loss-on-ignition, radionuclide activity, and inventory data, and ^{210}Pb age calculations for core 99928-1.

[Flux and inventory calculations completed by C.A. Rice; analytical data by M.E. Marot; --, not analyzed; **, not detected; dpm, disintegrations per minute]

Depth (cm)	Mean depth (cm)	Dry bulk density (g/cm^3)	Cumulative sediment weight (g/cm^2)	Loss-on-ignition (percent dry wt.)	Total ^{210}Pb activity (dpm/g)	Total ^{210}Pb activity error (± dpm/g)	Excess ^{210}Pb activity (dpm/g)[1]	Model date	Excess ^{210}Pb inventory (dpm/cm^2)[2]	^{226}Ra activity (dpm/g)	^{226}Ra activity error (±dpm/g)	^{137}Cs activity (dpm/g)	^{137}Cs activity error (± dpm/g)	^{234}Th activity (dpm/g)	^{234}Th activity error (± dpm/g)
0-1	0.5	0.273	0.273	20.20	12.68	0.17	11.127	1997	3.035	2.81	0.26	0.50	0.08	6.10	0.46
1-2	1.5	0.469	0.742	13.40	8.66	0.20	7.108	1994	3.336	--	--	--	--	--	--
2-3	2.5	0.610	1.352	10.80	6.14	0.08	4.590	1989	2.801	--	--	--	--	--	--
3-4	3.5	0.863	2.215	9.00	4.93	0.07	3.381	1983	2.918	2.81	0.20	0.67	0.07	4.67	0.38
4-5	4.5	0.828	3.043	10.80	6.74	0.08	5.194	1976	4.301	--	--	--	--	--	--
5-6	5.5	0.875	3.918	11.20	5.89	0.08	4.337	1970	3.793	--	--	--	--	--	--
6-7	6.5	0.741	4.659	9.00	3.84	0.06	2.291	1965	1.697	2.93	0.20	0.81	0.08	3.97	0.36
7-8	7.5	0.877	5.536	11.20	5.40	0.13	3.850	1958	3.376	--	--	--	--	--	--
8-9	8.5	0.763	6.299	9.40	4.41	0.06	2.865	1952	2.187	--	--	--	--	--	--
9-10	9.5	1.063	7.363	9.40	3.53	0.05	1.982	1945	2.108	2.71	0.21	0.19	0.05	3.76	0.38
10-12	11.0	0.903	9.168	7.60	3.26	0.05	1.712	1931	3.091	--	--	--	--	--	--
12-14	13.0	1.090	11.348	7.60	2.21	0.04	0.665	1915	1.450	--	--	--	--	--	--
14-16	15.0	1.104	13.556	4.40	1.68	0.03	0.132	1899	0.291	2.52	0.19	**	--	2.49	0.31
16-18	17.0	1.009	15.574	4.00	1.91	0.04	0.357	1884	0.720	--	--	--	--	--	--
18-20	19.0	1.030	17.634	4.20	1.51	0.03	-0.045	1868	0.000	--	--	--	--	--	--
20-22	21.0	1.051	19.736	4.00	1.76	0.03	0.213	1853	0.447	2.67	0.20	**	--	2.65	0.35
22-24	23.0	1.142	22.021	3.40	1.42	0.03	-0.128	1836	0.000	--	--	--	--	--	--
24-26	25.0	1.183	24.387	2.80	1.52	0.03	-0.029	1818	0.000	--	--	--	--	--	--
26-28	27.0	1.170	26.726	2.60	1.41	0.03	-0.144	1801	0.000	2.45	0.19	**	--	2.20	0.35
28-30	29.0	1.056	28.839	3.00	1.68	0.03	0.129	1786	0.272	--	--	--	--	--	--
30-32	31.0	1.130	31.098	3.20	1.71	0.04	0.161	1769	0.364	--	--	--	--	--	--
32-34	33.0	1.145	33.387	3.20	1.66	0.03	0.113	1752	0.259	2.61	0.18	**	--	2.40	0.32
34-36	35.0	1.106	35.600	2.20	1.37	0.03	-0.176			--	--	--	--	--	--
36-38	37.0	1.217	38.033	2.40	1.32	0.03	-0.226			--	--	--	--	--	--
38-40	39.0	1.177	40.386	3.20	1.35	0.03	-0.196			2.26	0.15	**	--	1.98	0.28
Bottom	41.0	1.155		2.80	1.42	0.03				--	--	--	--	--	--

[1]Excess ^{210}Pb activity is calculated by subtracting the average of the total ^{210}Pb activity from depth of 16 cm to bottom of core (1.55 dpm/g) from total ^{210}Pb activity.

[2]Excess ^{210}Pb Inventory = 35.55 dpm/cm^2 (from top of core down to core interval 20–22 cm, that is 150 years).

Table 8. Sample depths, loss-on-ignition data, radionuclide activity, and inventory data for core 99929-1.

[Flux and inventory calculations completed by C.A. Rice; analytical data by M.E. Marot; --, not analyzed; **, not detected; Tr, too low to quantify; dpm, disintegrations per minute]

Depth (cm)	Mean depth (cm)	Dry bulk density (g/cm^3)	Cumulative sediment weight (g/cm^2)	Loss-on-ignition (percent dry wt.)	Total ^{210}Pb activity (dpm/g)	Total ^{210}Pb activity error (± dpm/g)	Excess ^{210}Pb activity (dpm/g)	Excess ^{210}Pb inventory (dpm/cm^2)[1]	^{226}Ra activity (dpm/g)	^{226}Ra activity error (±dpm/g)	^{137}Cs activity (dpm/g)	^{137}Cs activity error (± dpm/g)	^{137}Cs inventory (dpm/cm^2)[2]	^{234}Th activity (dpm/g)	^{234}Th activity error (± dpm/g)
0-1	0.5	0.45	0.45	17.80	5.92	0.12	5.06	2.29	0.86	0.09	1.07	0.07	0.48	0.55	0.16
1-2	1.5	0.47	0.92	19.60	7.13	0.01	5.95	2.77	1.18	0.10	1.81	0.10	0.84	0.88	0.22
2-3	2.5	0.51	1.43	18.60	2.21	0.05	1.47	0.74	0.74	0.10	1.48	0.10	0.75	Tr	--
3-4	3.5	0.45	1.87	18.80	2.02	0.02	1.41	0.63	0.61	0.08	0.67	0.06	0.30	0.59	0.15
4-5	4.5	0.45	2.32	17.00	2.40	0.02	1.09	0.49	1.31	0.15	0.47	0.08	0.21	1.16	0.33
5-6	5.5	0.45	2.77	13.80	2.78	0.02	1.17	0.53	1.61	0.12	0.22	0.05	0.10	0.91	0.26
6-7	6.5	0.48	3.25	12.80	2.23	0.03	0.88	0.42	1.35	0.13	0.09	0.04	0.04	Tr	--
7-8	7.5	0.66	3.90	13.00	1.40	0.02	0.67	0.44	0.73	0.07	**	--		0.50	0.13
8-9	8.5	0.61	4.51	13.20	1.17	0.03	0.69	0.42	0.49	0.07	**	--		Tr	--
9-10	9.5	0.61	5.12	13.00	0.89	0.03	0.44	0.27	0.45	0.07	**	--		Tr	--
10-12	11	0.49	6.09	12.60	0.54	0.03	0.22	0.22	0.32	0.05	**	--		Tr	--
12-14	13	0.40	6.89	12.60	0.64	--	0.29	0.23	0.35	0.05	**	--		Tr	--
14-16	15	0.38	7.65	12.20	0.64	--	0.18	0.14	0.46	0.05	**	--		Tr	--
16-18	17	0.37	8.39	13.20	0.74	0.03	0.37	0.28	0.37	0.05	**	--		0.36	0.10
18-20	19	0.51	9.40	15.80	0.43	0.03	0.23	0.23	0.21	0.04	**	--		0.17	0.07
20-22	21	0.43	10.26	15.60	0.48	0.04			--	--	--	--		--	--
22-24	23	0.50	11.26	14.00	0.33	0.09			0.18	0.04	**	--		0.18	0.08
24-26	25	0.52	12.31	13.00	0.38	0.07			--	--	--	--		--	--
26-28	27	0.44	13.20	13.40	0.34	0.06			0.16	0.04	**	--		Tr	--
28-30	29	0.42	14.04	14.40	0.32	0.05			--	--	--	--		--	--
30-32	31	0.42	14.87	18.40	0.45	0.04			0.29	0.05	**	--		0.28	0.10
32-34	33	0.41	15.69	18.80	0.40	0.04			--	--	--	--		--	--
34-36	35	0.45	16.60	18.20	0.24	0.04			0.12	0.03	**	--		Tr	--
36-38	37	0.47	17.53	20.00	0.27	0.03			--	--	--	--		--	--
38-40	39	0.48	18.49	21.20	0.30	0.06			0.20	0.04	**	--		0.23	0.10
40-42	41	0.35	19.19	26.20	0.34	0.04			--	--	--	--		--	--
42-44	43	0.32	19.82	29.60	0.34	0.03			0.19	0.04	**	--		0.36	0.10
44-46	45	0.28	20.37	37.20	0.47	0.03			--	--	--	--		--	--
46-48	47	0.19	20.76	43.60	0.50	0.03			0.35	0.10	**	--		Tr	--
48-50	49	0.19	21.13	46.72	0.55	0.03			--	--	--	--		--	--
50-52	51	0.24	21.62	47.20	0.46	0.04			0.33	0.09	**	--		0.32	0.19
Bottom	53	0.14	21.89	35.99	1.49	0.02			0.45	0.09	**	--		0.84	0.24

[1]Excess ^{210}Pb Inventory = 9.0 dpm/cm^2 (from top of core down to core interval 10–12 cm where excess ^{210}Pb activity approaches a constant value).

[2]Inventory of ^{137}Cs = 2.73 dpm/cm^2.

Table 9. Sample depths, loss-on-ignition, radionuclide activity, and inventory data, and ^{210}Pb age calculations for core 99929-2.

[Flux and inventory calculations completed by C.A. Rice; analytical data by M.E. Marot; --, not analyzed; **, not detected; Tr, Trace quantity, too low to quantify; dpm, disintegrations per minute]

Depth (cm)	Mean depth (cm)	Dry bulk density (g/cm³)	Cumulative sediment weight (g/cm²)	Loss-on-ignition (percent dry wt.)	Total ^{210}Pb activity (dpm/g)	Total ^{210}Pb activity error (± dpm/g)	Excess ^{210}Pb activity (dpm/g)	Model date	Excess ^{210}Pb inventory (dpm/cm²)[1]	^{226}Ra activity (dpm/g)	^{226}Ra activity error (± dpm/g)	^{137}Cs activity (dpm/g)	^{137}Cs activity error (± dpm/g)	^{137}Cs inventory (dpm/cm²)[2]	^{234}Th activity (dpm/g)	^{234}Th activity error (± dpm/g)
0-1	0.5	0.076	0.076	32.95	31.47	0.58	29.41	1997	2.23	--	--	--	--	--	--	--
1-2	1.5	0.161	0.237	29.79	27.80	0.46	25.74	1994	4.15	--	--	--	--	--	--	--
2-3	2.5	0.218	0.455	26.60	24.20	0.34	22.14	1989	4.82	0.82	0.14	3.38	0.17	0.74	1.15	0.30
3-4	3.5	0.274	0.729	24.60	22.15	0.31	20.09	1984	5.50	0.95	0.15	3.62	0.17	0.99	1.30	0.33
4-5	4.5	0.264	0.992	23.60	18.81	0.28	16.75	1978	4.41	1.14	0.16	4.33	0.19	1.14	1.41	0.30
5-6	5.5	0.225	1.217	23.80	14.29	0.21	12.23	1973	2.75	1.13	0.16	4.75	0.20	1.07	1.59	0.37
6-7	6.5	0.284	1.502	26.20	13.05	0.24	10.99	1967	3.13	1.28	0.16	5.96	0.22	1.70	1.76	0.38
7-8	7.5	0.241	1.743	30.00	13.85	0.30	11.79	1962	2.84	1.24	0.19	8.78	0.30	2.12	1.74	0.45
8-9	8.5	0.315	2.058	34.60	14.48	0.23	12.42	1956	3.91	1.39	0.18	8.10	0.27	2.55	1.89	0.36
9-10	9.5	0.240	2.298	35.00	13.67	0.23	11.61	1951	2.79	1.26	0.20	6.06	0.28	1.46	1.77	0.50
10-12	11.0	0.175	2.649	40.60	12.22	0.25	10.16	1943	3.56	1.23	0.13	2.21	0.13	0.77	1.81	0.31
12-14	13.0	0.283	3.216	29.20	6.11	0.11	4.05	1931	2.30	1.77	0.16	0.55	0.08	0.31	2.62	0.39
14-16	15.0	0.263	3.741	34.20	5.14	0.11	3.08	1920	1.62	1.47	0.12	0.19	0.05	0.10	2.09	0.27
16-18	17.0	0.295	4.330	37.60	3.88	0.08	1.82	1908	1.07	1.18	0.12	Tr	--		1.63	0.26
18-20	19.0	0.259	4.848	43.80	3.77	0.07	1.71	1897	0.89	0.95	0.10	**	--		1.08	0.21
20-22	21.0	0.277	5.403	24.40	2.06	0.04	0.00	1885	0.00	--	--	--	--		--	--
22-24	23.0	0.323	6.049	37.00	3.28	0.12	1.22	1872	0.79	1.08	0.10	**	--		1.26	0.23
24-26	25.0	0.272	6.593	27.00	3.13	0.11	1.07	1860	0.58	--	--	--	--		--	--
26-28	27.0	0.282	7.158	49.20	4.24	0.08	2.18	1848	1.23	0.69	0.07	**	--		1.15	0.16
28-30	29.0	0.223	7.603	40.32	4.50	0.09	2.44	1839	1.09	--	--	--	--		--	--
30-32	31.0	0.322	8.247	37.60	3.71	0.07	1.65	1825	1.06	1.16	0.08	**	--		1.74	0.21
32-34	33.0	0.335	8.917	25.00	3.70	0.07	1.64	1811	1.10	--	--	--	--		--	--
34-36	35.0	0.369	9.655	25.60	4.13	0.09	2.07	1796	1.53	1.18	0.10	**	--		1.67	0.26
36-38	37.0	0.331	10.318	36.80	4.41	0.13	2.35	1782	1.56	--	--	--	--		--	--
38-40	39.0	0.152	10.622	70.60	14.87	0.26	12.81	1775	3.90	0.57	0.12	**	--		1.09	0.30
40-42	41.0	0.153	10.928	76.80	18.17	0.36	16.11	1769	4.92	--	--	--	--		--	--
42-44	43.0	0.196	11.320	63.80	9.93	0.21	7.87	1761	3.09	0.42	0.07	**	--		0.83	0.17
Bottom	44.5	0.112	11.543	53.80	12.22	0.24	10.16	1756	2.27	0.76	0.12	1.19	0.09		1.16	0.26

[1]Excess ^{210}Pb activity is calculated by subtracting the ^{210}Pb activity of 2.06 from total ^{210}Pb activity.

^{210}Pb Excess Inventory = 48.58 dpm/cm² (from top of core down to core interval 26–28 cm, that is 150 years).

[2] Inventory of ^{137}Cs = 12.95 dpm/cm².

Table 10. Sample depths, loss-on-ignition, radionuclide activity, and inventory data, and ^{210}Pb age calculations for core 99929-3.

[Flux and inventory calculations completed by C.A. Rice; analytical data by M.E. Marot; -- not analyzed; **, not detected; Tr, trace quantity, too low to quantify; dpm, disintegrations per minute]

Depth (cm)	Mean depth (cm)	Dry bulk density (g/cm^3)	Cumulative sediment weight (g/cm^2)	Loss-on-ignition (percent dry wt.)	Total ^{210}Pb activity (dpm/g)	Total ^{210}Pb activity error (± dpm/g)	Excess ^{210}Pb activity (dpm/g)[1,2]	Model date	Excess ^{210}Pb inventory (dpm/cm^2)[3]	^{226}Ra activity (dpm/g)	^{226}Ra activity error (± dpm/g)	^{137}Cs activity (dpm/g)	^{137}Cs activity error (± dpm/g)	^{137}Cs inventory (dpm/cm^2)[4]	^{234}Th activity (dpm/g)	^{234}Th activity error (± dpm/g)
0-1	0.5	0.058	0.058	18.40	13.47	0.20	11.55	1997	0.669	1.92	0.17	3.87	0.16	0.22	Tr	--
1-2	1.5	0.231	0.289	15.80	12.28	0.22	10.87	1990	2.511	1.41	0.21	2.96	0.19	0.68	1.15	0.35
2-3	2.5	0.319	0.608	13.20	10.43	0.28	8.39	1981	2.672	2.05	0.22	5.86	0.25	1.87	1.35	0.37
3-4	3.5	0.403	1.010	12.20	8.46	0.14	5.88	1968	2.368	2.58	0.18	6.52	0.22	2.63	1.30	0.35
4-5	4.5	0.555	1.565	8.60	6.03	0.09	3.63	1952	2.014	2.40	0.16	3.55	0.12	1.97	1.77	0.24
5-6	5.5	0.453	2.017	12.20	3.95	0.07	1.71	1938	0.775	2.23	0.18	1.50	0.10	0.68	1.11	0.26
6-7	6.5	0.286	2.303	15.20	3.33	0.07	0.60	1929	0.171	2.73	0.31	1.09	0.18	0.31	1.08	0.48
7-8	7.5	0.260	2.563	15.60	2.60	0.06	0.04	1921	0.009	2.56	0.23	0.52	0.11	0.14	1.02	0.39
8-9	8.5	0.261	2.824	13.80	2.19	0.05	-0.21	1913	0.000	2.40	0.28	Tr	--		Tr	--
9-10	9.5	0.328	3.153	12.40	2.36	0.05	0.20	1903	0.000	2.16	0.20	**	--		Tr	--
10-12	11.0	0.328	3.808	13.00	2.13	0.05	0.85	1884	0.558	1.27	0.09	0.06	0.03		0.32	0.11
12-14	13.0	0.282	4.373	12.80	1.19	0.04	0.65	1866	0.366	0.54	0.07	**	--		0.45	0.12
14-16	15.0	0.271	4.915	14.60	1.06	0.03	0.54	1850	0.290	0.53	0.08	**	--		0.59	0.17
16-18	17.0	0.238	5.392	11.75	0.92	0.02	0.38	1836	0.182	0.54	0.09	**	--		0.66	0.18
18-20	19.0	0.253	5.897	11.25	0.82	0.02	0.36	1820	0.184	0.46	0.08	**	--		0.49	0.15
20-22	21.0	0.332	6.562	29.00	0.75	0.02	0.15	1800	0.097	--	--	--	--		--	--
22-24	23.0	0.186	6.935	43.20	1.61	0.03	0.87	1789	0.325	0.74	0.10	**	--		1.34	0.21
24-26	25.0	0.170	7.274	43.80	1.40	0.03	0.73	1779	0.248	--	--	--	--		--	--
26-28	27.0	0.194	7.661	59.60	1.76	0.04	1.17	1767	0.451	0.59	0.08	**	--		0.99	0.17
28-30	29.0	0.156	7.974	61.60	1.80	0.05	1.17	1757	0.366	--	--	--	--		--	--
30-32	31.0	0.175	8.324	58.60	1.92	0.05	1.26	1747	0.443	0.66	0.09	**	--		1.09	0.22
32-34	33.0	0.181	8.686	49.60	1.60	0.04	0.96	1736	0.348	--	--	--	--		--	--
34-36	35.0	0.283	9.251	49.40	1.76	0.09	1.13	1719	0.641	0.62	0.07	**	--		0.88	0.16
36-38	37.0	0.354	9.958	24.60	0.90	0.02	0.35	1697	0.250	--	--	--	--		--	--
38-40	39.0	0.170	10.297	61.40	1.67	0.04	1.20	1687	0.406	0.47	0.07	**	--		1.17	0.16
40-42	41.0	0.162	10.622	67.50	1.70	0.04	1.27	1677	0.412	--	--	--	--		--	--
42-44	43.0	0.153	10.928	65.25	1.73	0.04	1.34	1668	0.409	0.39	0.12	**	--		0.41	0.24
44-46	45.0	0.247	11.422	64.40	1.89	0.05	1.44	1653	0.711	--	--	--	--		--	--
46-48	47.0	0.129	11.679	62.40	1.50	0.04	0.98	1645	0.252	0.52	0.11	**	--		0.77	0.25
48-50	49.0	0.198	12.076	60.60	1.19	0.03	0.69	1633	0.272	--	--	--	--		--	--
50-52	51.0	0.198	12.472	64.20	1.50	0.04	1.01	1621	0.399	0.49	0.07	**	--		0.81	0.15
52-54	53.0	0.189	12.850	60.80	1.22	0.03	0.65	1610	0.246	--	--	--	--		--	--
54-56	55.0	0.196	13.241	65.00	1.67	0.03	1.03	1598	0.404	0.64	0.07	**	--		0.81	0.16
56-58	57.0	0.165	13.572	65.20	1.56	0.04	0.96	1588	0.317	--	--	--	--		--	--
58-60	59.0	0.189	13.950	60.80	1.53	0.04	0.93	1576	0.352	0.60	0.09	**	--		0.92	0.21
60-62	61.0	0.202	14.355	56.00	2.34	0.06	1.742	1564	0.705		--	--	--		--	--
Bottom	63.5	0.275	14.905	--	--	--	--	--		--	--	**	--		1.49	0.22

[1]Excess ^{210}Pb activity is calculated by subtracting the ^{226}Ra activity from total ^{210}Pb activity. For intervals with no ^{226}Ra activity, an interpolated activity was used from the mean of the adjacent intervals.

[2]Excess ^{210}Pb activity calculated using value of 0.60 from 59–60 cm.

[3]Inventory of ^{210}Pb = 12.4 dpm/cm^2 (from top of core down to core interval 14–16 cm, that is 150 years).

[4]Inventory of ^{137}Cs = 8.49 dpm/cm^2.

^{210}Pb Radiometric Calculations

The chemical systematics affecting the accumulation of ^{210}Pb in the Animas River watershed require that the radionuclides be in equilibrium with ambient ^{226}Ra, and assume that there is a constant flux of excess ^{210}Pb, f (dpm/cm^2/yr), and mass of sediment, r (g/cm^2/yr). Figures 4–6, which are log-linear plots of total ^{210}Pb versus cumulative sediment weight, indicate these assumptions are reasonable considering the type of environment. Perturbations from straight-line decay of ^{210}Pb are primarily from variations in organic content in the cores, which trap the radionuclides more effectively. Because of the influence of ground water in lower portions of some of the cores and the variable and sometimes high organic content of the cores, the excess ^{210}Pb, which is the difference between total ^{210}Pb and ^{226}Ra, was calculated using constant values of ^{226}Ra in two of the cores. In the other core, the difference between total ^{210}Pb and the measured ^{226}Ra was used.

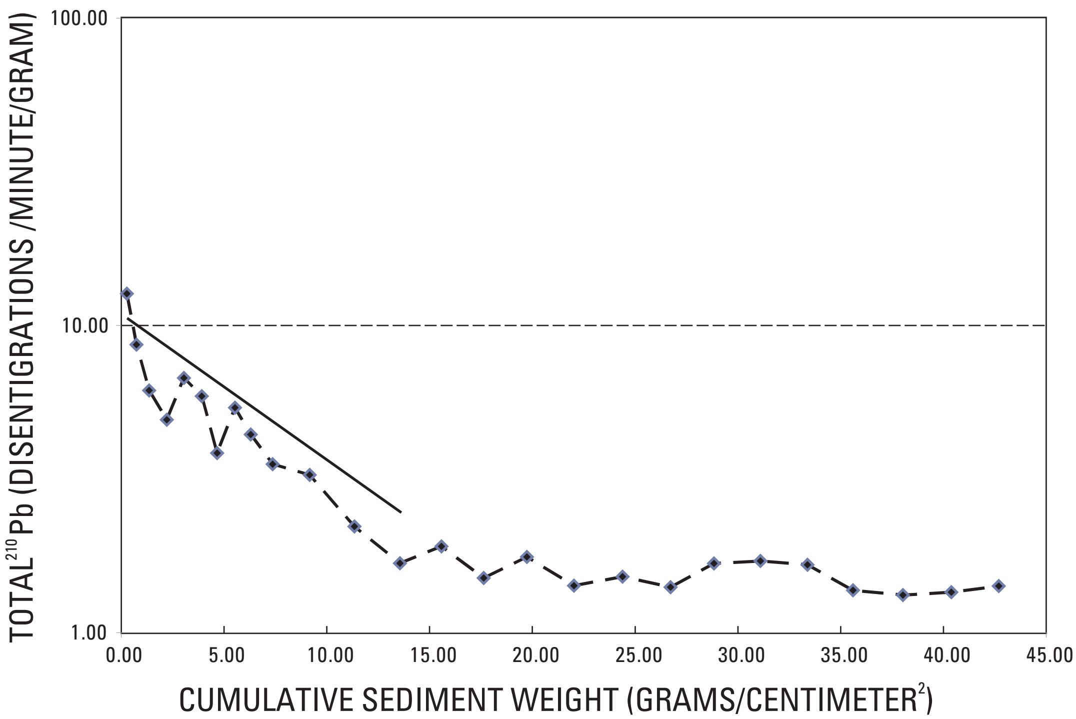

Figure 4. Log-linear plot of total ^{210}Pb activity versus the cumulative sediment weight for core 99928-1 (table 7). Straight line shows exponential decay of ^{210}Pb assuming constant rates of supply of ^{210}Pb and mass.

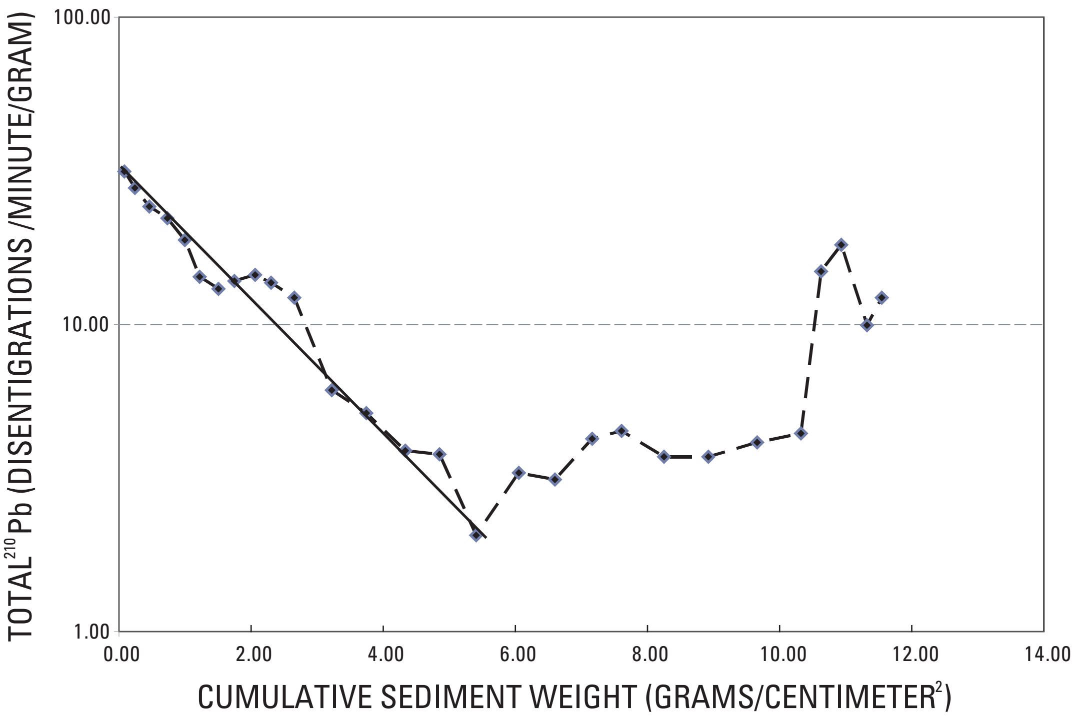

Figure 5. Log-linear plot of total ^{210}Pb activity versus the cumulative sediment weight for core 99929-2 (table 9). Straight line shows exponential decay of ^{210}Pb assuming constant rates of supply of ^{210}Pb and mass.

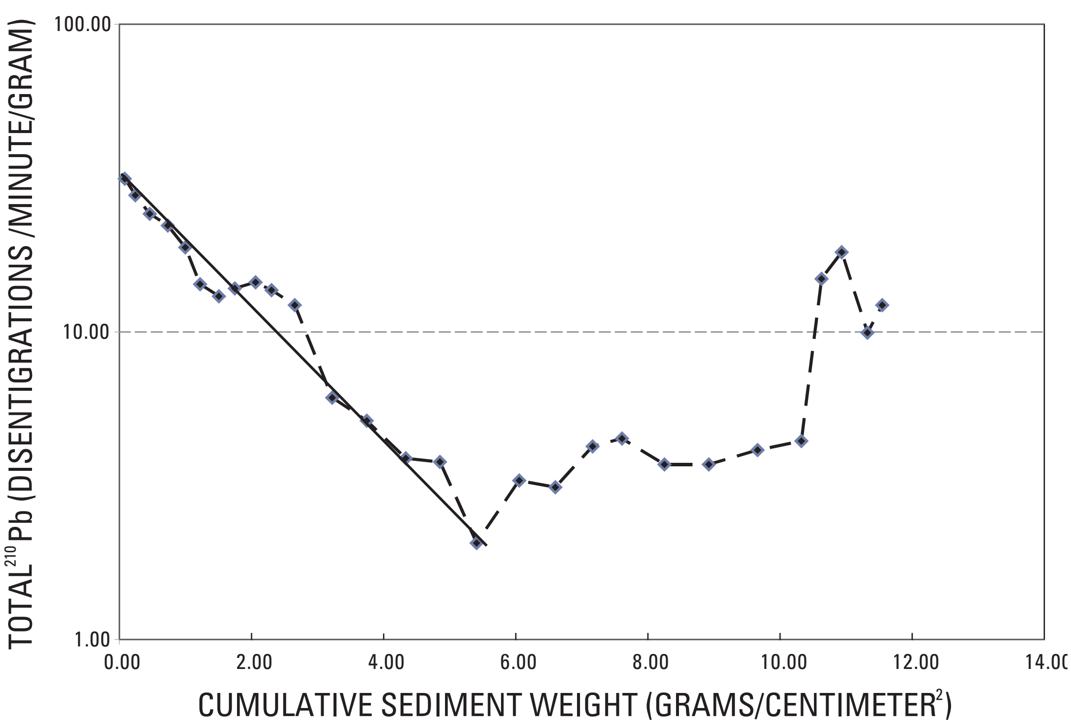

Figure 6. Log-linear plot of total ^{210}Pb activity versus the cumulative sediment weight for core 99929-3 (table 10). Straight line shows exponential decay of ^{210}Pb assuming constant rates of supply of ^{210}Pb and mass.

The excess activity (A_{ex}) of ^{210}Pb is the result of the exponential decay of the excess ^{210}Pb at time zero, A_o: $A_{ex}=A_o e^{-\lambda t}$, where λ is the radioactive decay constant (λ=0.03114 yr^{-1}), A_o=f/r, and t=g/r, where g (g/cm^2) is the cumulative weight of sediment at a given depth. Ages of sediment can be calculated from g/r. By using the cumulative sediment weight rather than core depth, effects of compaction are taken into account. Statistical counting errors given in tables 7–10 are the major source of error. For this study, samples were counted for a period of time to provide less than 5 percent counting error, thus the calculated ages have a ±5 percent error. This translates to ±2.5 years at 50 years B.P.

Individual cores were analyzed by calculating a best-fit curve to the excess ^{210}Pb data and the cumulative sediment weight using an unweighted Marquardt-Levenberg parameter optimization method (Press and others, 1989). A distinct advantage of this procedure over other methods used to reduce ^{210}Pb data is that all data points are used in the sediment-accumulation-rate calculations, including negative values (which are the result of statistical counting errors in the deeper parts of the sediment column where there is a small signal-to-noise ratio). This method has the further advantage of eliminating the mathematical consequence that produces "old age errors" and a null ^{210}Pb disequilibria that is inherent in other best-fit interpolation routines. Null ^{210}Pb disequilibria mathematically yield an infinitely old age, a geologic impossibility. Analytical results and an alternative age model for core 99929-2 are presented in table 9.

The ^{210}Pb age model for each core was compared with the ^{137}Cs activity peak, which was assumed to be 1963 ± 2 years. The calculated ^{210}Pb ages agree well with the age calculated from the ^{137}Cs activity peak.

Geochemical Influence of Periodic Flooding of the Oxbow Lakes, Durango Area

Water level records for the lower Animas River reach indicate that the oxbow lakes in the Durango, Colo., area are occasionally flooded in the spring whenever the flow exceeded 8,000 cubic feet per second (cfs). Flood stages are tabulated in table 11 from stream flow data obtained largely from the stream gage at the 32nd Street Bridge located immediately downstream from the site (fig. 2). Observations of the water level during the May 2005 flood showed that a flow of 8,000 cfs resulted in bank-full flow at the site (fig. 2). On the basis of these flow records, flood deposition of sediment from overbank sheet flow in these oxbow lakes should not have occurred since 1949, and had probably only occurred 8 to 10 times between 1897 and 1949 (table 11). The largest flood events were the 500-year flood in 1911 and two large floods in 1927. Because the floodplain area in which the oxbow lakes reside is flat and marshy, detritus from local erosion deposited in the oxbow lakes would be minimal. Overbank flow sampled during the May 2005 flood shows that the river had a very small suspended-sediment load by the time it had reached 8,000 cfs. Thus, the inorganic sediment deposited within the oxbow lake is dominated by wind-blown detritus derived largely from sediment on the exposed riverbed at low flow.

Table 11. Discharge records from NWIS gage 09361500, 32nd St. Bridge, Durango, Colo.

Flood year	Dates discharge >7,000 cfs (no records from this gage during period—*in italics*)	Peak discharge ft^3/sec (estimated peak discharge—*in italics*)
1909	*Sept. 24*	*10,000*
1911	*Oct. 5–11*	*25,000*
1914	June 2	8,330
1917	June 14–24	8,460
1920	May 21–June 2	9,260
1921	June 10-16	9,300
1922	June 10	7,000
1927	*June 29*	*20,000*
1927	*Sept. 10–13*	*14,000*
1941	May 13–16	9,500
1948	May 20	7,500
1949	June 18–21	10,700
1952	June 8–11	7,550
1957	June 5, 6	8,090
1970	Sept. 6	7,400
1973	June 11, 12	7,110
1979	May 28–30	7,480
1979	June 7	7,260
1980	June 10–12	7,550
1984	May 24, 25	7,070
1985	June 9	7,250
2005	May 22–25	8,070

References Cited

Briggs, P.H., 2002, The determination of forty elements in geological and botanical samples by inductively coupled plasma–atomic emission spectrometry, chap. G *of* Taggart, J.E., ed., Analytical methods for chemical analysis of geologic and other materials: U.S. Geological Survey Open-File Report 02-223, 18 p.

Buxton, H.T., Nimick, D.A., von Guerard, Paul, Church, S.E., Frazier, Ann, Gray, J.R., Lipin, B.R., Marsh, S.P., Woodward, Daniel, Kimball, Briant, Finger, Susan, Ischinger, Lee, Fordham, J.C., Power, M.S., Bunck, Christine, and Jones, J.W., 1997, A science-based, watershed strategy to support effective remediation of abandoned mine lands: Fourth Annual International Conference on Acid Rock Drainage Proceedings, v. IV, Vancouver, B.C., Canada, May 31–June 5, 1997, p. 1,869–1,880.

Church, S.E., 1981, Multielement analysis of fifty-four geochemical reference samples using inductively coupled plasma–atomic emission spectrometry: Geostandards Newsletter, v. 5, p. 133–160.

Church, S.E., Mosier, E.L., and Motooka, J.M., 1987, Mineralogical basis for the interpretation of multielement (ICP–AES), oxalic acid, and aqua-regia partial digestions of stream sediments for reconnaissance exploration geochemistry: Journal of Geochemical Exploration, v. 29, p. 207–233.

Church, S.E., von Guerard, Paul, and Finger, S.E., 2007, eds., Integrated investigations of environmental effects of historical mining in the Animas River watershed, San Juan County, Colorado: U.S. Geological Survey Professional Paper 1651, 1,096 p.

Crock, J.G., Lichte, F.E., and Briggs, P.H., 1983, Determination of elements in National Bureau of Standards geologic reference materials SRM 278 obsidian and SRM 688 basalt by inductively coupled plasma–atomic emission spectroscopy: Geostandards Newsletter, v. 7, p. 335–340.

Cutshall, N.H., Larsen, I.L., and Olsen, C.R., 1983, Direct analysis of ^{210}Pb in sediment samples: Self-adsorption corrections: Nuclear Instrumental Methods Physics Research, v. 26, p. 309–312.

Ferderer, D.A., 1996, National overview of abandoned mine land sites utilizing the minerals availability system (MAS) and geographic information systems (GIS) technology: U.S. Geological Survey Open-File Report 96-549, 42 p.

Fey, D.L., Unruh, D.M., and Church, S.E., 1999, Chemical data and lead isotopic compositions in stream-sediment samples from the Boulder River watershed, Jefferson County, Montana: U.S. Geological Survey Open-File Report 99-575, 147 p. [http://pubs.usgs.gov/of/1999/ofr-99-0575/].

Fey, D.L., Church, S.E., and Unruh, D.M., 2000, Geochemical and lead isotopic data from sediment cores, fluvial tailings, iron bogs, and pre-mining terrace deposits, Animas River watershed, Colorado, 1995–1999: U.S. Geological Survey Open-File Report 2000-0465, 13 p. [http://pubs.usgs.gov/of/2000/ofr-00-0465/].

Flynn, W.W., 1968, The determination of polonium-210 in environmental materials: Analytica Chimica Acta, v. 43, p. 121–131.

Jones, W.R., 2007, History of mining and milling practices and production in San Juan County, Colorado, 1871–1991, *in* Church, S.E., von Guerard, Paul, and Finger, S.E., eds., Integrated investigations of environmental effects of historical mining in the Animas River watershed, San Juan County, Colorado: U.S. Geological Survey Professional Paper 1651, p. 39–86.

National Institute of Standards and Technology (NIST), 1993a, Certificate of analysis standard reference material 2704, Buffalo River sediment: National Institute of Standards and Technology.

National Institute of Standards and Technology (NIST), 1993b, Certificate of analysis standard reference material 2709, San Joaquin soil: National Institute of Standards and Technology.

National Institute of Standards and Technology (NIST), 1993c, Certificate of analysis standard reference material 2710, contaminated Montana soil: National Institute of Standards and Technology.

National Institute of Standards and Technology (NIST), 1993d, Certificate of analysis standard reference material 2711, Montana soil: National Institute of Standards and Technology.

Press, W.H., Flannery, B.P., Teukolsky, S.A., and Vetterling, V.T., 1989, Numerical recipes: The art of scientific computing: New York, Cambridge University Press, 234 p.

Robbins, J.A., Holmes, C.W., Halley, R.B., Bothner, M.A., Shinn, E.A., Graney, J., Keeler, G., TenBrink, M., Orlandini, K.A., and Rudnick, D.E., 2000, Time-averaged flux of lead and fallout radionuclides to sediment in Florida Bay: Journal of Geophysical Research, v. 105, p. 28,805–28,821.

Runnells, D.D., Shephard, T.A., and Angino, E.E., 1992, Metals in water—Determining natural background concentrations of dissolved components in water at mining, milling, and smelting sites: Mining Engineering, v. 50, p. 65–71.

Taggart, J.E., Jr., Lindsay, J.R., Scott, B.A., Vivit, D.V., Bartel, A.J., and Stewart, K.C., 1987, Analysis of geologic materials by wavelength-dispersive X-ray fluorescence spectrometry, *in* Baedecker, P.A., ed., Methods for geochemical analysis: U.S. Geological Survey Bulletin 1770, p. E1–E19.

USDA Forest Service and Bureau of Land Management, 2007, Abandoned mine lands: A decade of progress reclaiming hardrock mines: Forest Service Publication No. FS-891 and BLM Publication No. BLM-WO-GI-07-013-3720, 33 p. [http://www.fs.fed.us/geology/aml-index.htm and http://www.blm.gov/aml].

U.S. Geological Survey, 1898, Topographic map of the Durango quadrangle: U.S. Geological Survey, scale: 1:250,000.

U.S. Geological Survey, 1997, A plan for the USGS abandoned mine lands initiative, 1997–2001: U.S. Geological Survey web page [http://amli.usgs.gov/amli/5year/, accessed February 15, 2007].

Wilson, S.A., Briggs, P.H., Mee, J.S., and Siems, D.F., 1994, Determination of thirty-two major and trace elements in three NIST soil SRMs using ICP–AES and WDXRF: Geostandards Newsletter, v. 18, p. 58–89.

Publishing support provided by:
Denver Publishing Service Center

For more information concerning this publication, contact:
Team Chief Scientist, USGS Central Mineral Resources
Box 25046, Mail Stop 973
Denver, CO 80225
(303)236-1562

Or visit the Central Mineral Resources Team Web site at:
http://minerals.cr.usgs.gov/

USGS

Church and others—**Radionuclide Data from Cores of the Animas River, Colorado**—Data Series 382

Printed on recycled paper